

The Pitting Corrosion Behavior of Copper with Different Grain Size

Yanhui Ma^{1,*}, Xiaoxuan Tian², Jianfeng Yin¹, Junping Chen¹, Jianan Jiang^{3,*}

¹ North China Electric Power Institute Co.,Ltd, Beijing 100045, China

² Xi'an Thermal Power Research Institute Co.,Ltd, Xi'an 710003, China

³ Department of materials science and engineering, University of sheffield, Sheffield, S1 3JD, UK

*E-mail: mayanhui1985@163.com, 420030973@qq.com

Received: 3 January 2019 / Accepted: 13 February 2019 / Published: 10 April 2019

In this paper, the pitting corrosion behaviours of copper materials with different grain sizes (average grain sizes of 23, 67, and 470 μm) were investigated based on cyclic polarization and electrochemical impedance spectroscopy (EIS). The results showed that a very protective passive film without any pitting can be observed in NaOH solutions. The pitting corrosion behaviours were observed in a Na_2SO_4 solution and a $\text{Na}_2\text{SO}_4 + \text{NaOH}$ solution. The pitting susceptibility of copper decreased with the increasing grain size in the Na_2SO_4 solution due to a decrease in the electrochemically active surface area. In contrast, the pitting susceptibility increased with increasing copper grain size in the $\text{Na}_2\text{SO}_4 + \text{NaOH}$ solution, which was related to a decrease in the quality of the formed passive film.

Keywords: Copper; Pitting corrosion; Grain size; Cyclic polarization; Electrochemical impedance spectroscopy

1. INTRODUCTION

It is well known that the grain sizes of metal materials have a remarkable influence on the performance of a material, such as the mechanical properties and corrosion behaviour [1]. Currently, there has been an extensive amount of research on the correlations between the grain size and the corrosion performance of different materials (such as Al [2], Ni [3], Zn [4], Mg [5], Ti [6], Co [7], Ni-W [8] and stainless steel [9]). A number of researchers have claimed that a reduction in the grain size would considerably improve the corrosion performance due to modification of the cathodic reaction processes, decreases in the localized attack that occurs at the grain boundaries or the rapid formation of a continuous and protective passive film [3-4, 7]. Alternatively, numerous other studies have demonstrated that a decrease in grain size would reduce corrosion resistance. It has been found that inter-

crystalline defects (such as grain boundaries) would be the preferential corrosion path. A decrease in grain size would increase the anodic dissolution of the active sites, resulting in an acceleration of the corrosion [2, 10]. Therefore, the correlation between grain size and corrosion resistance is an intricate and important issue and has attracted extensive interest [11-17].

Copper and its alloys are the most important industrial materials with a wide variety of applications because of their excellent electrical, thermal and mechanical properties and corrosion resistances [18]. The copper workpieces used in many industries are always exposed to different environments, such as copper condenser pipes in high-temperature environments. These conditions may cause unavoidable evolution of the crystal structures and grain sizes [19-20]. Specifically, pitting often occurs at the grain boundaries of copper, which may be one of the primary reasons for the failure of copper workpieces [22]. However, research on the effects of the grain size on the pitting corrosion behaviour of copper have rarely been reported. In this paper, we use an annealing treatment to regulate the grain sizes of copper samples. Furthermore, the pitting corrosion resistances of copper samples with different grain sizes were evaluated by cyclic polarization and EIS in conjunction with the equivalent circuit analysis.

2. EXPERIMENTAL

Polycrystalline copper (99.97%) was employed in this study. Rectangular samples, with a strict area of 1 cm×1 cm, were prepared from copper ingots by electrical discharge machining. Then, the samples were polished to a mirror-like finish and ultrasonically cleaned with acetone and distilled water. Finally, the annealing treatment was performed under a hydrogen atmosphere at 200 °C, 600 °C, and 1000 °C for 3 h.

The microstructures at the surfaces of the copper samples were characterized by optical microscopy (DM2500M) after etching in a solution of 50 g of FeCl₃ in 100 mL of CH₃CH₂OH and 5 mL of a 37% HCl solution. After the electrochemical experiments, the surface morphologies of the corrosion products were observed by scanning electron microscopy (SEM) by using a JEOL JSM-6700F microscope.

All electrochemical measurements were carried out in a conventional three-electrode cell containing a saturated calomel reference electrode (SCE), a platinum plate as the counter-electrode, and the copper samples with different grain sizes as the working electrode. The surface area of the copper samples exposed to the electrolyte was 1 cm². The test solutions were 0.1 M NaOH, 0.1 M Na₂SO₄ and 0.1 M Na₂SO₄+ 0.1 M NaOH.

The cyclic polarization experiments were performed at a scan rate of 30 mV min⁻¹. Tests were begun below the corrosion potential (-0.3 V) and scanned in the electropositive direction until reaching a potential of 1.2 V; then, the scans were reversed and continued to -0.2 V. After cyclic polarization, copper samples were immersed in a given solution until a steady open circuit potential was recorded. Then, EIS tests were carried out from 10⁵ Hz to 10⁻² Hz with a 5 mV amplitude signal. All solutions used in this paper were prepared from reagent grade chemicals and doubly distilled water, and each electrochemical test was repeated at least three times at 25±0.1 °C to confirm the reproducibility of the experimental data.

3. RESULTS AND DISCUSSION

3.1 Microstructure

As shown in Fig. 1, the average grain sizes of the copper specimens, which were annealed at 200 °C, 600 °C and 1000 °C, are determined to be approximately 23 μm , 67 μm , and 470 μm , respectively. In addition, no crystal orientations or unique textures are observed in the microstructures of the samples. In this paper, these samples are denoted as Cu-23, Cu-67, and Cu-470, according to their approximate grain sizes.

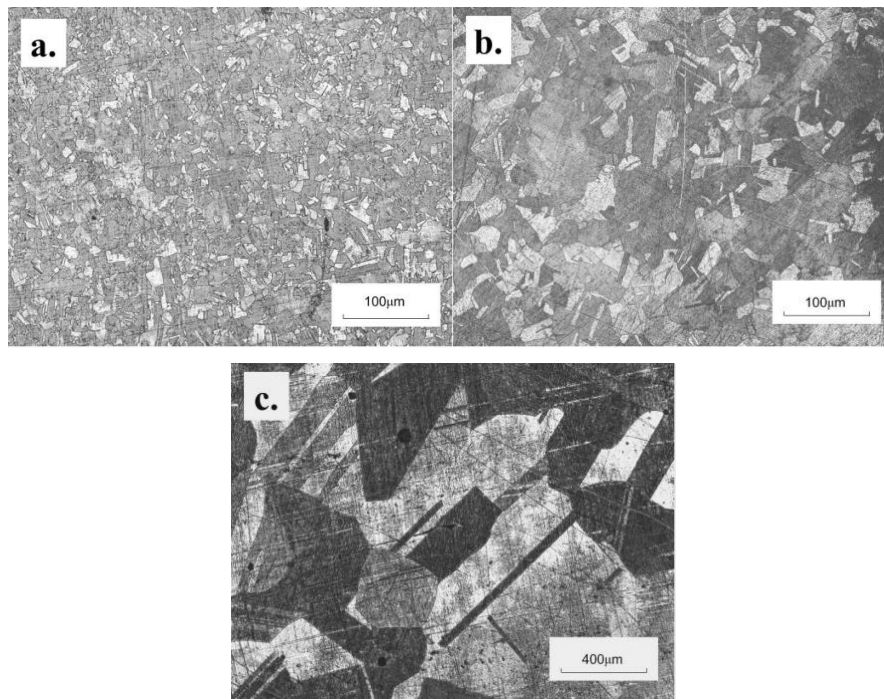
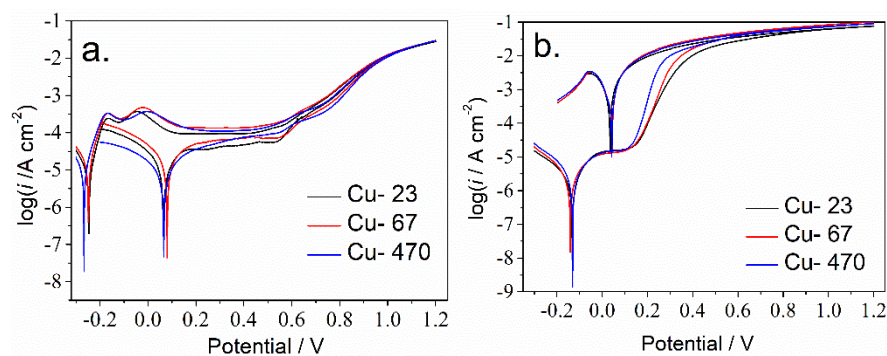


Figure 1. Metallographic photos of copper specimens annealing at different temperatures (a, 200 °C; b, 600 °C; c, 1000 °C)

3.2. Cyclic polarization analysis



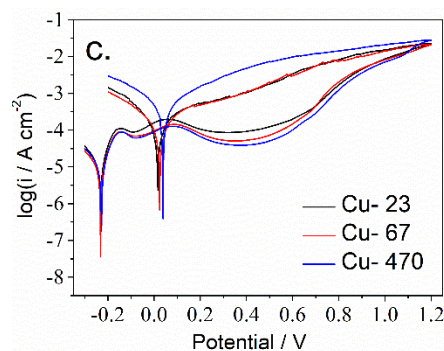


Figure 2. Cyclic polarization curves of copper specimens in different solutions (a, 0.1 M NaOH; b, 0.1 M Na₂SO₄; c, 0.1 M Na₂SO₄ + 0.1 M NaOH)

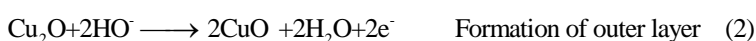
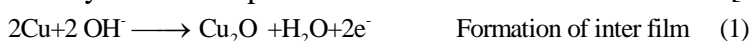
Cyclic polarization (or pitting scans) allows for qualitatively interpreting the pitting corrosion and ascertaining the electrochemical parameters of the pitting corrosion, such as the pitting potential (E_{pit}) and repassivation potential (E_{rp}). The cyclic polarization can be used to predict the corrosion behaviour of the metal samples in the given solutions by forcing the metal out of the steady state condition and then removing the force and returning, at a constant rate, to the steady state condition [23].

Fig. 2 shows the cyclic polarization curves of the copper samples in the different solutions. The corresponding electrochemical parameters extracted from Fig. 2 are listed in Table 1. The shapes of the cyclic polarization curves are approximately similar for samples in the same solution, while there is a substantial difference among the electrochemical behaviours of the copper samples in different solutions.

Table 1. Corresponding electrochemical parameters extracted from Fig. 2

Solution	Samples	E_{corr} (V)	I_{corr} (A cm ⁻²)	E_{pit} (V)	E_{rp} (V)
NaOH	Cu-23	-0.247	6.16×10^{-6}	0.583	-
	Cu-67	-0.250	8.55×10^{-6}	0.536	-
	Cu-470	-0.267	1.10×10^{-5}	0.534	-
Na ₂ SO ₄	Cu-23	-0.129	1.02×10^{-6}	0.141	0.036
	Cu-67	-0.139	1.34×10^{-6}	0.129	0.040
	Cu-470	-0.129	1.77×10^{-6}	0.114	0.041
Na ₂ SO ₄ + NaOH	Cu-23	-0.233	3.02×10^{-6}	0.505	0.068
	Cu-67	-0.228	3.89×10^{-6}	0.484	0.063
	Cu-470	-0.231	4.16×10^{-6}	0.476	0.048

The cyclic polarization curves of the copper samples in the NaOH solution are shown in Fig. 2a. All the curves exhibit partially stable current densities in the anodic polarization region, suggesting that protective passive films have formed on the copper surface. Generally, the passivity of copper has been identified as forming a dual-layered oxide structure, which consists of an outer CuO/Cu(OH)₂ layer and an inner Cu₂O film [24, 25]. The main process of formation for the duplex layer is as follows, and the inner Cu₂O layer acts as a protective barrier to inhibit corrosion [16, 26-27]:



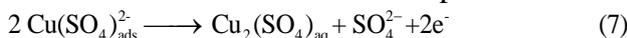


Complete reversibility of the current during the reverse potential scans of the cyclic polarization curves was found for the NaOH solution (Fig. 2a), which indicated the absence of any localized corrosion during the cyclic polarization test [28]. In addition, it can be seen that the passive current density (i_{pass}) decreases with decreasing grain size, indicating that fine grain sizes improve the passivating abilities of copper and form stable and protective passive films in the NaOH solution.

In the Na_2SO_4 solution (Fig. 2b), at the initial stage of the anodic polarization, a narrow passivating region is observed. In this narrow region, the plateau of the current density is caused by the adsorbed species ($\text{Cu}(\text{SO}_4)_{\text{ads}}^{2-}$ and $\text{Cu}(\text{OH})_{\text{ads}}^-$) formed on the electrode surface according to reactions (4)–(6) [29–31]:



In addition, the current density increases when the anodic potential is greater than the E_{pit} , which is due to the dissolution of the adsorbed species according to the following reactions (7)–(8) [31]:



Furthermore, the value of E_{tp} is more negative than that of E_{pit} , indicating that pitting will occur on the electrode surface [32]. The area of the hysteresis loop (S_{loop}), which can be used to assess the pitting tendency, was estimated from equation (9) [33]:

$$S_{\text{loop}} = \int_{E_{\text{tp}}}^{1.2\text{V}} (\log i_2 - \log i_1) \quad (9)$$

where i_1 and i_2 represent the current densities from the forward scanning curve and backward scanning curve, respectively. Fig. 3 shows the S_{loop} of the copper samples as a function of the grain sizes. It can be found that the value of S_{loop} decreases with increasing grain size, which demonstrates that pitting corrosion is less sensitive and there is a lower rate of pit formation in the Na_2SO_4 solution. According to previous studies, sulfate ions will accelerate the electro-dissolution and solubilizing of the products in the anodic process in neutral Na_2SO_4 -containing aqueous solutions [34]. The susceptibility to formation and propagation of the pits increases with decreasing grain size, which is likely due to an increase in the number of grains per unit area, resulting in an increase in the electrochemically active surface area available for pit nucleation, and the faster kinetics of formation for Cu-oxide dissolution and pit growth.

In the 0.1 M Na_2SO_4 +0.1 M NaOH mixed solution (Fig. 2c), hysteresis in the cyclic polarization curve can be observed during the negative potential scan along with the localized breakdown of the passivity. In this solution, competitive adsorption between the hydroxyl and sulfate ions plays an important role in the early stages of Cu-oxide layer formation, the mixture of soluble Cu-oxide species in the passive film can induce a breakdown of the copper passivity and pitting corrosion. In addition, the value of S_{loop} increases as the grain size increases (Fig. 3). The localized corrosion resistance increases with decreasing grain size, showing a tendency opposite to that in the Na_2SO_4 solution. This demonstrates that the effect of the grain size on the pitting corrosion rate may be dominated by the passive film properties.

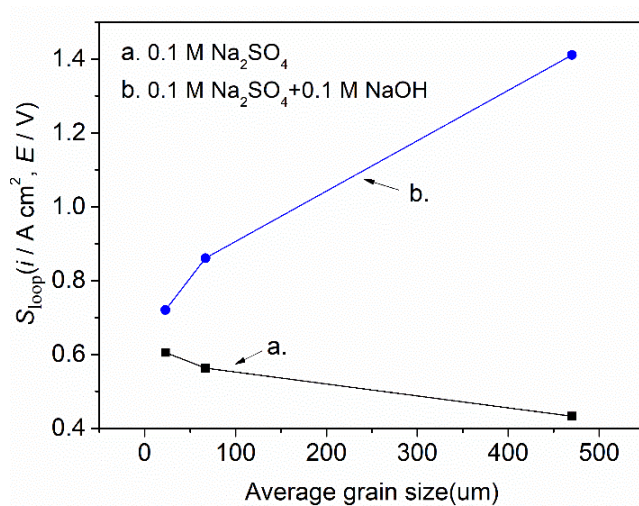


Figure 3. The S_{loop} of copper specimens as a function of grain size variation

3.3 EIS measurements and equivalent circuit analysis

EIS, a non-destructive technique for investigating the electrochemical reactions at the electrode/electrolyte interface, was employed to confirm the corrosion behaviour [35]. The EIS plots are shown in Fig. 4. Obviously, the impedance values of the samples in the NaOH solution are larger than those in the Na₂SO₄ solution and Na₂SO₄ + NaOH solution. Furthermore, the impedance values of the samples in the Na₂SO₄ solution are the smallest of the three solutions. In addition, the corrosion behaviours are different in the different solutions. In the NaOH solution (Fig. 4a-b), the impedance of the copper samples increases with decreasing grain sizes, indicating that the grain size can facilitate the formation of a high-quality passive film in the NaOH solution. In addition, the phase angles in the low and medium frequency regions are close to 90°, signifying that the samples are highly passivated and that passive films with low conductivities, which can act as protective layers to prevent further corrosion, are formed [36]. In the Na₂SO₄ solution (Fig. 4c-d), the impedances of the copper samples decrease with decreasing grain sizes, indicating that a decrease in the grain size would decrease the corrosion resistance. In addition, two time constants are observed, of which the time constant in the intermediate-frequency range represents the dielectric characteristic of the copper substrate, and the time constant in the low-frequency range corresponds to the formed pits. In the Na₂SO₄ + NaOH solution (Fig. 4e-f), the impedances of the copper sample increase with decreasing grain sizes, exhibiting a similar trend as that for the NaOH solution. In addition, there is only one time-constant, which is similar to that of the NaOH solution. However, the phase angles are lower and decrease into the low-frequency range due to the SO₄²⁻ ion accelerating the dissolution of the passive film [37].

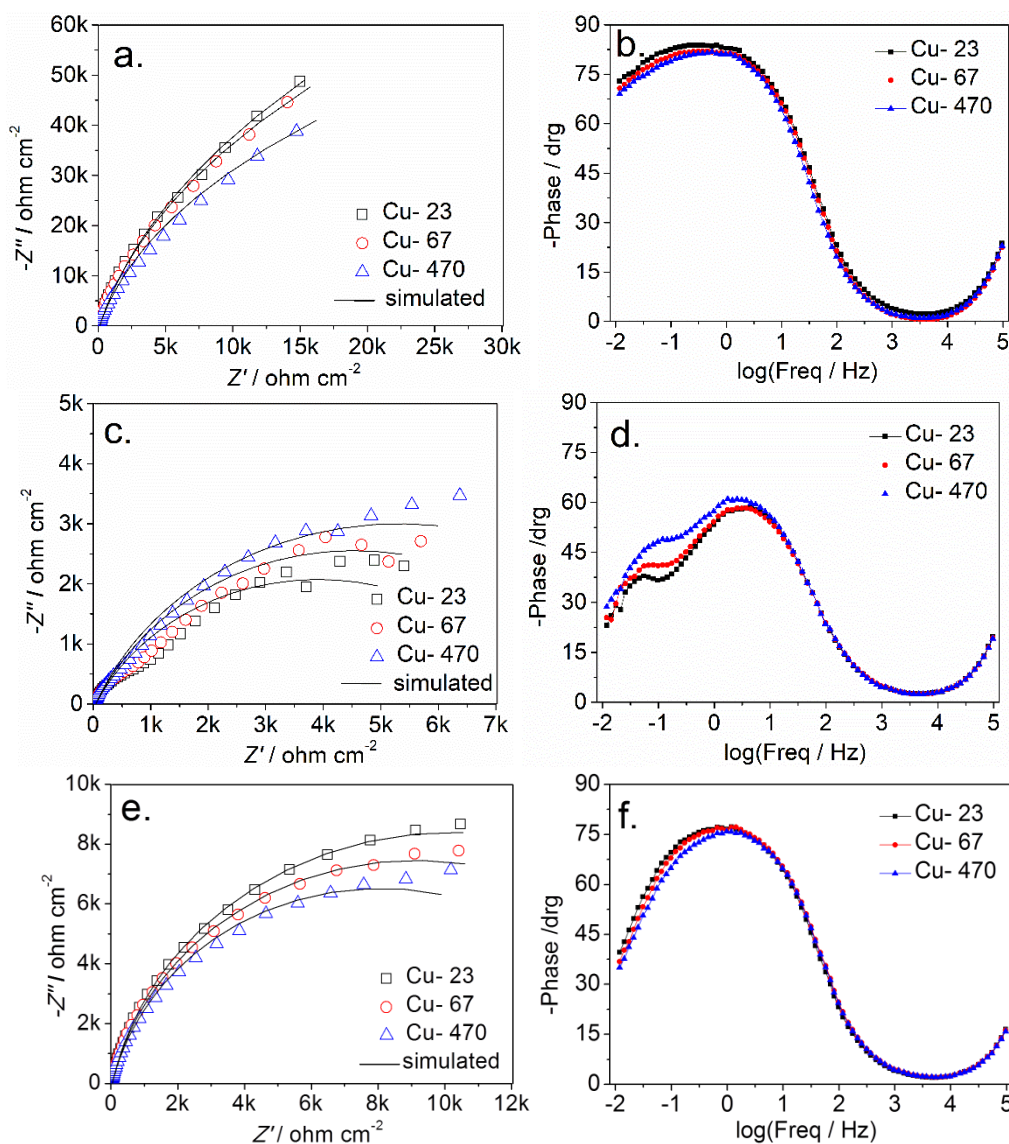


Figure 4. The EIS plots of copper specimens in different solutions (a, b: 0.1 M Na₂SO₄; c, d: 0.1 M NaOH; e, f: 0.1 M Na₂SO₄ + 0.1 M NaOH)

Fig. 5 shows the SEM images of the copper surfaces after the EIS measurements. No visible pitting can be observed on the surfaces of the copper samples in the NaOH solution (Fig. 5a). The diameters of the pits that formed in the Na₂SO₄ solution are 15~ 50 μm (Fig. 5b). In the case of the samples in the Na₂SO₄+NaOH mixed solution, a thin layer with numerous small perforations formed over the pits, which had diameters of 250 μm, as presented in Fig. 5c, which is larger than the pits shown in Fig. 5b. The residue of the passive film surrounding the pits played a key stabilizing role by containing the local aggressive environment of the pits. Therefore, the passive performance of the samples is a key factor in the film breakdown. These surface states from the EIS results and SEM images strongly agree with the results obtained from the cyclic polarization measurements.

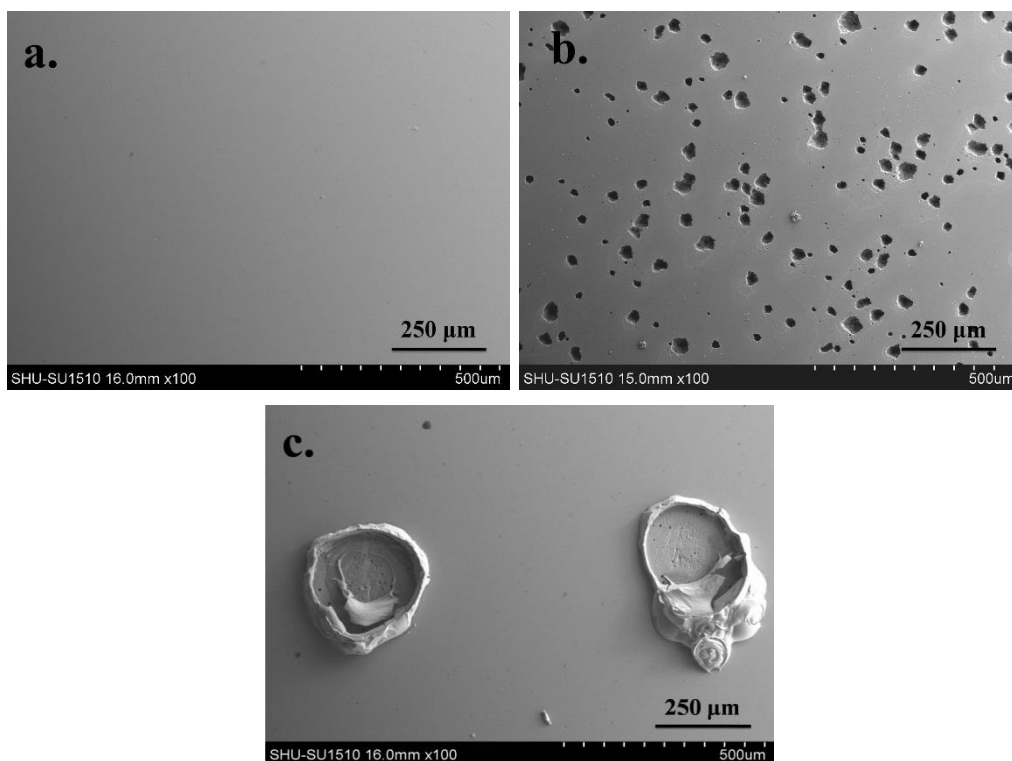


Figure 5. Typical micrographs of copper specimens after electrochemical measurements (a, 0.1 M Na_2SO_4 ; b, 0.1 M NaOH ; c, 0.1 M Na_2SO_4 + 0.1 M NaOH)

The equivalent impedance circuit shown in Fig. 6 was used to model the electrode and the electrolyte interface [38]. Here, R_s is the solution resistance, R_t is the charge-transfer resistance, and CPE represents the total capacitance of the constant phase-angle element. As shown in Fig. 4, the fitting lines are quite similar to the experimental EIS plots, indicating that the obtained electrochemical parameters listed in Table 2 can explain the corrosion behaviours of the electrode/electrolyte interface.

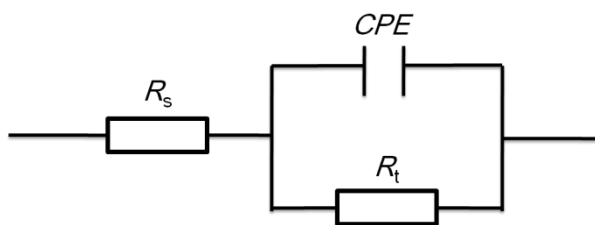


Figure 6. The equivalent circuit for fitting the EIS plots

As shown in Table 2, the R_t value in NaOH solution at least 10-times bigger than that in other solutions, suggesting the stronger protective passive films formed in moderate alkaline solutions. In Na_2SO_4 solution or Na_2SO_4 + NaOH mixed solution the small R_t value in confirm that their low resistance of localized corrosion. However, a distinct difference was observed in these two solutions. In neutral Na_2SO_4 solutions, the R_t value decrease individually in the order $\text{Cu-23} < \text{Cu-67} < \text{Cu-470}$, which indicates that the anti-pit corrosion resistance enhance with the increase of grain size. While R_t value

decreases as grain size increases in Na₂SO₄+ NaOH mixed solution, Cu-23 shows the highest resistance to the pit corrosion.

Table 2. Equivalent circuit parameters for the copper specimen in different solution

Solution	Samples	R_s (ohm cm ⁻²)	Y_0 -CPE (F cm ⁻²)	n_c	R_{ct} (ohm cm ⁻²)
NaOH	Cu-23	27.91	2.08×10^{-4}	0.927	2.77×10^5
	Cu-67	26.74	2.13×10^{-4}	0.928	2.45×10^5
	Cu-470	28.59	2.35×10^{-4}	0.924	1.73×10^5
Na ₂ SO ₄	Cu-23	19.43	6.98×10^{-4}	0.728	6.44×10^3
	Cu-67	19.50	6.91×10^{-4}	0.734	7.48×10^3
	Cu-470	18.07	6.93×10^{-4}	0.762	8.80×10^3
Na ₂ SO ₄ + NaOH	Cu-23	15.21	4.64×10^{-4}	0.879	2.04×10^4
	Cu-67	15.15	4.39×10^{-4}	0.874	1.82×10^4
	Cu-470	15.14	4.51×10^{-4}	0.869	1.61×10^4

In addition, it can be found that the n values for the CPE of copper are remarkably different for the different solutions. The CPE can reflect the non-ideal dielectric properties of the electrode surface [39]. In the Na₂SO₄ solution, the values of n are 0.728~0.762, indicating a porous electrode surface with corrosion pits. In contrast, for the NaOH solution, the values of n are 0.924~0.928, indicating weakly conductive passive films on the electrode surface without any pitting. However, in the 0.1 M Na₂SO₄+0.1 M NaOH mixed solution, the n value deviates from that of an ideal capacitor, suggesting passive film breakdown and the appearance of localized corrosion. These results are consistent with the analysis of the cyclic polarization data and SEM micrographs.

4. CONCLUSIONS

In this paper, the pitting corrosion behaviours of copper samples with different grain sizes (average grain sizes of 23, 67, and 470 μm) were studied. The results show that the grain size has different influences on the corrosion behaviour of copper for different solutions:

(1). In the NaOH solution, a very protective passive film without any pitting is formed on the copper surface. The passive current density decreases and the impedance increases with decreasing grain size.

(2) In the Na₂SO₄ solution, the pitting susceptibility increases with decreasing grain sizes due to an increase in the electrochemically active surface area available for pit nucleation and the higher kinetics of formation for Cu-oxide dissolution and pit growth.

(3) In the Na₂SO₄ + NaOH solution, the effect of the grain size on pitting corrosion may be dominated by passive film breakdown; smaller grain sizes show improved resistances to pitting corrosion.

ACKNOWLEDGEMENTS

This paper is financially supported North China Electric Power Institute Co.,Ltd and Xi'an Thermal Power Research Institute Co.,Ltd.

References

1. S. Gollapudi, *Corros. Sci.*, 62 (2012) 90.
2. K.D. Ralston, D. Fabijanac and N. Birbilis, *Electrochim. Acta*, 56 (2011) 1729.
3. R. Mishra and R. Balasubramaniam, *Corros. Sci.*, 46 (2004) 3019.
4. N.N. Aung and W. Zhou, *Corros. Sci.*, 52 (2010) 589.
5. H.S. Kim, S. J. Yoo, J.W. Ahn, D.H. Kim and W.J. Kim, *Mat. Sci. Eng. A.*, 528 (2011) 8479.
6. S. H. Kim, K.T. Aust, U. Erb, F. Gonzalez and G. Palumbo, *Scripta. Mater.*, 48 (2003) 1379.
7. A. Chianpairot, G. Lothongkum, C. A. Schuh and Y. Boonyongmaneerat, *Corros. Sci.*, 53 (2011) 1066.
8. K. H. Hou, Y. F. Chang, S. M. Chang and C. H. Chang, *Thin. Solid. Films*, 518 (2010) 7535.
9. S.X. Li, Y.N. He, S.R. Yu and P.Y. Zhang, *Corros. Sci.*, 66 (2013) 211.
10. E. E. Oguzie, S. G. Wang and Y. Li, *J. Solid. State. Electrochem.*, 12 (2008) 721.
11. A. M. Alfantazi, T. M. Ahmed and D. Tromans, *Mater. Design*, 30 (2009) 2425.
12. E. M. Pinto, A. S. Ramos, M. T. Vieira and C. M. A. Brett, *Corros. Sci.*, 52 (2010) 3891.
13. X. X. Xu, F. L. Nie, J. X. Zhang, W. Zheng, Y. Zheng, C. Hu and G. Yang, *Mater. Lett.*, 64 (2010) 524.
14. H. Miyamoto, K. Harada, T. Mimaki, A. Vinogradov and S. Hashimoto, *Corros. Sci.*, 50 (2008) 1215.
15. P. Shi, Q. Wang, Y. Xu and W. Luo, *Mater. Lett.*, 65 (2011) 857.
16. W. Luo, Y. Xu, Q. Wang, P. Shi and M. Yan, *Corros. Sci.*, 52 (2010) 3509.
17. A. Poursae, *Electrochim. Acta*, 55 (2010) 1200.
18. X. Leng, Y. Zhang, Q. Zhou, Y. Zhang, Z. Wang, H. Wang and B. Yang, *Mater. Res. Express.*, 5 (2018) 056513.
19. F. S. Afonso, M. M. M. Neto, M. H. Mendonça, G. Pimenta, L. Proença and I. T. E. Fonseca, *J. Solid. State. Electrochem.*, 13 (2009) 1757.
20. B. Yu, P. Woo and U. Erb, *Scripta. Mater.*, 56 (2007) 353.
21. Q. Zhou, S. Sheikh, P. Ou, D. Chen, Q. Hu, and S. Guo, *Electrochem. Commun.*, 98 (2019) 63.
22. Q. Zhou, J. Jiang, Q. Zhong, Y. Wang, K. Li and H. Liu, *J. Alloy. Compd.*, 563 (2013) 171.
23. H. Ibrahim, S. Mohammed and A. Amin, *Int. J. Electrochem. Sci.*, 5 (2010) 278-294.
24. S. Sathiyarayanan, M. Sahre and W. Kautek, *Corros. Sci.*, 41 (1999) 1899.
25. Q. Zhou, S. Liu, L. Gan, X. Leng and S. Wei, *Mater. Res. Express*, 5 (2018) 116534.
26. Y. Li, J.B He, M. Zhang and X.L. He, *Corros. Sci.*, 74(2013) 116.
27. J. Kunze, V. Maurice, L.H. Klein, H.H. Strehlow and P. Marcus, *J. Phys. Chem. B*, 105 (2001) 4263.
28. W. Ye, Y. Li and F. Wang, *Electrochim. Acta*, 51 (2006) 4426.
29. D. Šatović, L.V. Žulj, V and S. Martinez. *Corros. Sci.*, 51(2009) 1596.
30. E. Hamed, *Mater. Chem. Phys.*, 121(2010) 70.
31. K. M. Ismail, A. M. Fathi and W. A. Badawy, *Corrosion*, 60(2004) 795.
32. H. Luo, Z. Li, A.M. Mingers and D. Raabe, *Corros. Sci.*, 134 (2018) 131.
33. K. H. Lo, C. H. Shek and J. K. L. Lai, *Mat. Sci. Eng. R.*, 65 (2009) 39.
34. R. M. Souto, S. González, R. C. Salvarezza and A. J. Arvia, *Electrochim. Acta*, 39(1994) 2619.
35. A. Robin, G. A. S. Martinez and P. A. Suzuki, *Mater. Design*, 34 (2012) 319.
36. Q. Zhou, Y. Wang, H. Wu, Q. Zhong and J. Jiang, *Surf. Coat. Tech.*, 207 (2012) 503.
37. M. Scendo, *Corros. Sci.*, 49(2007)3953.
38. W. R. Osório, L.C. Peixoto, M. V. Canté and A. Garcia, *Electrochim. Acta*, 55 (2010) 4078.
39. Q. Zhou, W. Xie, Y. Zhang, M. Sheng, A. Hu and L. Zhang, *Surf. Rev. Lett.*, 24 (2017) 1850015.